Synthesis, Characterization and Evaluation of Corrosion Inhibition Potencial of a novel Schiff Base for carbon steel in acidic environment

Luana B. Furtado[1], Pedro H. C. dos Santos[1], Maria José O. C. Guimarães[1], Rafaela C. Nascimento[2], Peter R. Seidl[1], Janaína C. Rocha[1], José Antônio C. P. Gomes[1]

[1]Federal University of Rio de Janeiro – UFRJ, Rio de Janeiro, Brazil

[2]Centro de Química de Évora, University of Evora – Évora, Portugal

luana_bf18@hotmail.com, cpedrohenriques@gmail.com, rafaelan@uevora.pt

***Abstract*— Corrosion remains a serious problem since steel is used in most industrial sectors. It costs billions of dollars each year, especially in industrial processes that expose metal to acidic fluids. Among the methods of corrosion protection, using inhibitors is a common and important tool. Schiff bases are organic compounds containing $R_2C=NR$, which forms a complex with metal ions through coordination bonds. They have proven to be cheap starting precursors with a relatively easy synthetic route. In this context, the objective of this paper was to synthesize an aniline based imine, N,N-dimethyl-4-[(phenylimino)methyl]aniline (SB) and access its corrosion inhibition potential in the protection of API P110 carbon steel alloy in 1M HCl. SB was prepared from aniline and 4-(dimethylamino)benzaldehyde by condensation reaction. The Schiff base crystals were analyzed using Fourier-transform infrared spectroscopy (FTIR) and Proton nuclear magnetic resonance (^{1}H NMR). For gravimetric analysis, API P110 coupons were submitted to weight loss tests in 1M HCl solution in the presence of the inhibitor at concentrations of 100, 350 and 600 ppm, and temperatures of 303, 318 and 333 K. The statistical design (2^2) revealed that temperature showed a high influence on the response Corrosion rate (CR, mm/y), indicating that changing the concentration of SB affects the CR much less than changing the temperature. The best inhibition efficiency obtained from weight loss, 92.28%, was achieved using 600 ppm of SB at 318 K, with a corrosion rate of 2.00 mm per year. The Langmuir isotherm model best represented the adsorption results, with a R^2 value of 0.9952. This informs that the adsorption is characterized by a monolayer coverage of the metal surface. The Gibbs free energy change of adsorption value, ΔG_{ads}, showed that adsorption of the inhibitor is spontaneous and characterized by physisorption. The Activation Energy values, E_a, obtained from the Arrhenius equation corroborates the physical-type adsorption. Confocal laser microscopy showed pits in the coupons tested with the inhibitor that corresponded to moderate localized corrosion.**

Keywords—corrosion; inhibitor; carbon steel; Shiff base.

I. INTRODUCTION

Corrosion remains a serious problem since steel is used in most industrial sectors. It costs billions of dollars each year, especially in industrial processes when metal is exposed to acidic fluids [1]. Carbon steel is the most widely used engineering material due to its good mechanical properties and low cost. It is used in several applications such as transportation, chemical processing, petroleum production and refining, pipelines and construction. The exposure of carbon steel to different, severe and variable industrial conditions, such as temperature and pH, can result in direct and indirect costs related to the corrosion process [2]. Among the methods of corrosion protection, using inhibitors is a common and important method. Normally, the corrosion inhibitor is added to the acidic environment in order to control the corrosion of metallic structures. Between organic compounds, aromatic heterocyclic compounds containing N, S, O and π-electrons have high potential to be considered as corrosion inhibitors. Common organic inhibitors are from the family of amides, imides (Schiff bases), imidazolines, nitrogen quaternaries, polyoxyalkylated amines, salts of nitrogenous molecules with carboxylic acids, or nitrogen heterocyclics [3,4]. Schiff bases are organic compounds containing $R_2C{=}NR$, which forms an indeterminate complex with metal ions through coordination bonds [5]. Imines are particularly common as intermediates in many biological pathways. The amino acid alanine, for instance, is metabolized in the body by reaction with the aldehyde pyridoxal phosphate (PLP), a derivative of vitamin B6, to yield a Schiff base that is further degraded [6]. They have proven to be cheap starting precursors with relatively easy synthetic route. The high purity, low toxicity and eco-friendliness have made the synthesis and structural studies of new Schiff base compounds very interesting. In the last few years, extensive efforts have been made, both in academics and industry to develop Schiff base compounds with interesting anti-corrosion effect, because of their thermal stability, complex forming ability and semiconducting properties [7]. There are three main types of Schiff base corrosion inhibitors used for corrosion protection of carbon steel: complex type Schiff base inhibitors, heterocyclic Schiff base inhibitors and aniline Schiff base inhibitors.

The authors thank Conselho Nacional de Desenvolvimento Científico e Tecnológico – CNPq, Brazil, for sponsoring.

Fig. 1. Condensation reaction used to produce the Shiff base N,N-dimethyl-4-[(phenylimino)methyl]aniline (SB) from aniline and 4-(dimethylamino)benzaldehyde.

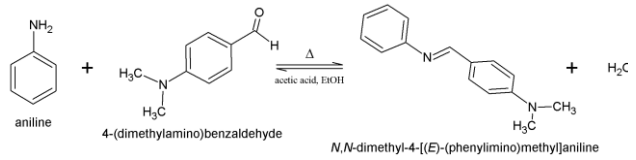

Previous studies have shown that the Schiff base corrosion inhibitors have excellent adsorption performance on carbon steel and prevent corrosion by effectively forming a dense protective layer [5]. In this context, the objective of this paper was to synthesize an aniline based imine, N,N-dimethyl-4-[(phenylimino)methyl]aniline (SB) and access its corrosion inhibitor potential in the protection of API P110 carbon steel alloy in 1M HCl. The nucleophilic addition reaction is the most common general reaction type for aldehydes and ketones. Many kinds of products can be prepared by nucleophilic additions. Schiff bases are produced when primary amines add to carbonyl compound, in which water is eliminated from the initially formed tetrahedral intermediate and a new C=N double bond is formed. Imines are formed in a reversible, acid-catalyzed process that begins with nucleophilic addition of the primary amine to the carbonyl group, followed by transfer of a proton from nitrogen to oxygen to yield a carbinolamine. Protonation of the carbinolamine oxygen by an acid catalyst then promotes the loss of water, which produces an iminium ion. Loss of a proton from nitrogen gives the final product and regenerates the acid catalyst [6]. Figure 1 shows the global reaction used to synthesize the Schiff base, aim of this study.

II. EXPERIMENTAL

A. Synthesis of SB

For the imine preparation, equimolar quantities of aniline and 4-(dimethylamino)benzaldehyde (ACS reagent, 99%, Sigma-Aldrich) were dissolved in anhydrous ethanol (99,8%, Sigma-Aldrich), and then mixed with glacial acetic acid, to a final volume of 200 mL, in which the acid catalyst and ethanol proportion was 1:5 v/v. The mixture was heated and refluxed for 2 hours. After reaction, the resulting mixture was recrystallized 3 times in anhydrous ethanol for purification. Then, the solids were weighted and dried until constant weight was obtained.

B. Characterization of the Schiff Base

The Schiff base crystals were analyzed using Fourier-transform infrared spectroscopy (FTIR) and Proton nuclear magnetic resonance (^{1}H NMR). The aniline used as reagent was also analyzed by FTIR for comparation. The FTIR analysis was performed using a Thermo Scientific Nicolet is5 Fourier-transform infrared spectrometer, at 293 K. In total, 20 scans were collected from 4000 to 650 cm^{-1} and resolution of 4.00 cm^{-1}. The Proton Nuclear Magnetic Resonance analysis was conducted in a Varian Mercury VX 300 spectrometer, at 313 K. The Schiff base (10 – 15 mg) was solubilized in 0.8 mL of deuterated chloroform (CIL 99.8% d). Observation frequency: 299.99 MHz. Number of scans: 20. Interval between pulses (delay-d1): 20 s. Data were obtained with MestreNova software version 11.04 using Fourier Transform.

C. Corrosion Inhibitor Potential Analysis

1) Experimental Design: A two level factorial statistics design, 2^2, with 2 replicas on the central point, was used to define the influence of the factors on the corrosion inhibition potential of the Shiff base. The factors evaluated were the Schiff base concentration (100, 350 and 600 ppm) and temperature (303, 318 and 333 K). The dependent variable chosen was the Corrosion Rate (CR, mm/y). The data analysis was executed using the software Statistica (version 13.4.0.14), with a 95% trust (α = 0,05). Table I shows the experimental conditions performed. Each table cell marked green represents a test performed in that value of temperature and inhibitor concentration. Also, two test coupons were used in each condition (duplicates) and avarage values were taken for the mass loss studies.

TABLE I. GRAVIMETRIC CORROSION TEST CONDITION POINTS[A]

		Temperature (K)		
		303	***318***	***333***
Concentration (ppm)	***0***	1	1	1
	100	1		1
	350	1	2	1
	600	1		1

[A] Green marked table cells refer to a test executed under that condition. The number in each cell represents the number of tests executed in that condition. Only the central point was performed twice.

2) Gravimetric Corrosion Tests: In order to access the potential of SB as a corrosion inhibitor, API P110 coupons with the following composition (%wt): C, 0.280; Mn, 1.220; Si, 0.280; P, 0.016; S, 0.002; Ni, 0.010; Mo, 0.110; and Fe, 98.1, were submitted to weight loss tests in 1M HCl solution in the presence of the inhibitor at concentrations of 100, 350 and 600 ppm, and temperatures of 303, 318 and 333 K. Two extra conditions of 350 ppm of inhibitor at 303 and 333 K were also performed in order to use in the adsorption studies. Prior to the corrosion tests, the coupons were prepared by abrading on aluminum oxide sandpapers (mesh 220, 360 and 600, in this order), washed in distilled water, degreased in acetone, and then dried, according to [8]. After weighting the test coupons with a 0.1 mg sensitivity, the coupons were placed in 300 mL autoclaves. After 24 h exposure to the acidic environment, the coupons were taken out from the autoclaves, rinsed thoroughly with distilled water, dried and weighted again. Final mass was obtained for each coupon after several chemical cleaning steps using Clarke's solution for removing residual corrosion products from the coupons' surfaces. Weight loss results were used to calculate the uniform corrosion rate (CR), the inhibition efficiency (IE) and to obtain the adsorption mechanism and its parameters.

Fig. 2. $_1$H NMR spectrum of the synthesis products.

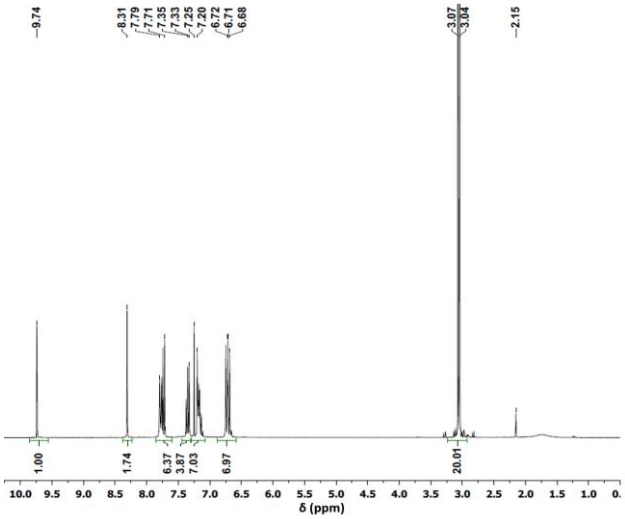

Fig. 3. FTIR spectra. In blue, the imine product spectrum; in red, aniline.

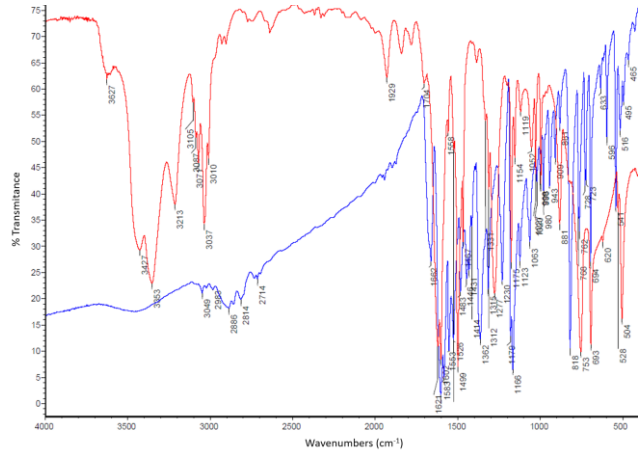

D. *Surface Analysis – Confocal laser scanning microscopy*

The API P110 carbon steel coupon surfaces were analyzed by Confocal laser scanning microscopy (CLSM) in a ZEISS LSM 800 MAT with Zen 2.3 Blue edition software. The coupons were submitted to weight loss measurements in the absence (blank) and presence of the inhibitor (600 ppm, 318 K). After 24 h, they were cleaned and scanned by CLSM.

III. Results and Discussion

A. *Substances characterization*

The Schiff base was characterized by FTIR and ^{1}H NMR. While FTIR reveals the types of functional groups present in a molecule, RMN provides information about the number of atoms magnetically distinct of the studied isotope (^{1}H, in this case). The combination of the FTIR and NMR data, is, most times, just enough to completely identify the structure of an unknown molecule [9]. Figure 2 shows the proton NMR spectrum for the imine-based products from the synthesis. The proton NMR showed an intense doublet peak for chemical shifts (δ) of 3.04 and 3.07 ppm, referring to the ∫–N–$(CH_3)_2$ hydrogens. Peaks between δ of 6.68 ppm and 7.79 ppm refer to aromatic H, from the two aromatic rings of the SB. The peak at δ 8.31 ppm refers to the imine hydrogen, ∫–N═CH–∫. This peak confirms the formation of the Schiff base from the amine and aldehyde condensation reaction. The peak at 9.74 ppm might refer to the 4-(dimethylamino)benzaldehyde carbonyl hydrogen ∫–COH from unreacted aldehyde, given its very similar chemical shift values.

The aniline IR spectrum, in red, shows characteristic aniline bands at 3427 and 3353 cm^{-1}, due to the N–H stretches of primary amines, and also presents its shoulder band at 3213 cm^{-1}. The N–H bend band is presented at 1621 cm^{-1}. The N–H bond of primary and secondary amines shows up at 753 cm^{-1}. The SB IR spectrum, blue, shows bands at 2714 and 2814 cm^{-1}, most probably the C–H stretches from the aldehyde structure. The medium intensity band at 1662 cm^{-1}, close to the 1621 cm^{-1} N–H bend band, present in both spectra, refers to the C=N imine bond stretch, confirming the formation of the SB.

B. *Experimental Design*

The Pareto chart, Figure 4(A), shows that the only significant factor is the temperature and that neither concentration, and the ratio between temperature and concentration are significant. Curvature was also not a significant factor. In this sense, the relation between the factors and corrosion rate is linear. The pure error obtained by ANOVA test was 0.0450, and the lack of fit was 12.67. Figure 4(B) shows the observed vs. predicted values from the model obtained, and it indicated a good adjustment of the data. Figure 5 presents the fitted response surface, showing how temperature and concentration of inhibitor influence the corrosion rate.

Fig. 4. In (A), Pareto chart of standardized effects for CR (mm/y) as response; In (B), Observed vs. Predicted values chart for CR (mm/y).

(A)

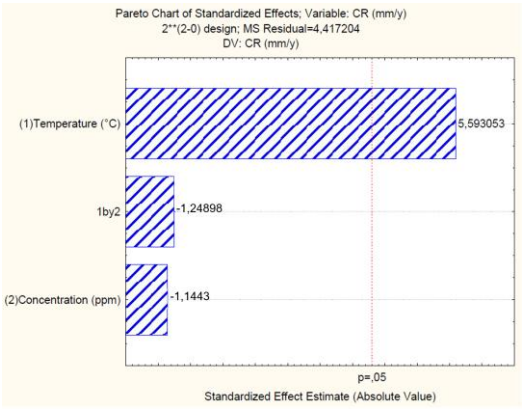

(B)

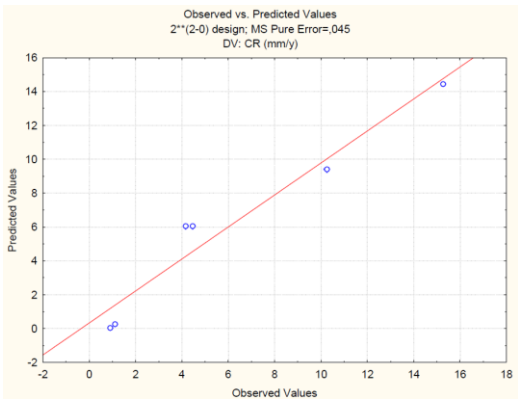

Fig. 5. Response surface for CR (mm/y).

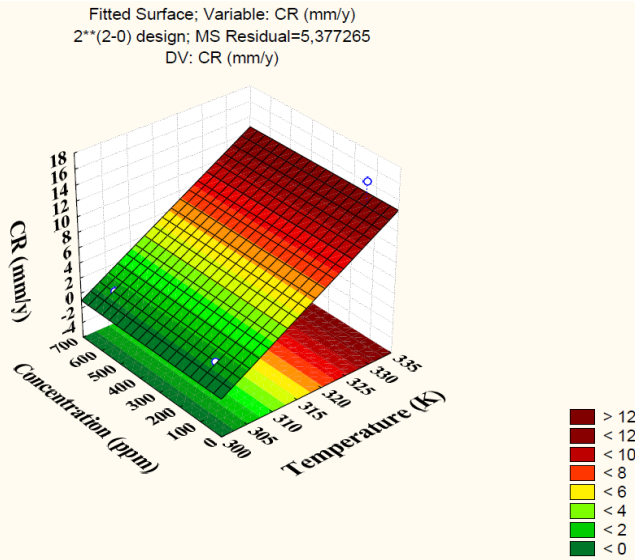

The surface of response shows that increasing the temperature significantly increases the corrosion rate, despite the concentration of inhibitor. The inhibitor concentration is statistically not effective in influencing the response variable, as seen on the Pareto chart.

C. Gravimetric Measurements

The corrosion rates (CR), in mm/y, and the inhibition efficiencies (IE, %) of the corrosion tests performed at 303, 318 and 333 K are shown in Table II.

TABLE II. CORROSION RATE AND INHIBITION EFFICIENCY FOR API P110 IN 1M HYDROCLORIC ACID IN THE ABSENCE AND PRESENCE OF DIFFERENT CONCENTRATIONS OF SB, AT 303, 318 AND 333 K.

SB Concentration ($mg \cdot L^{-1}$)	303K		318K		333K	
	CR (mm/y)	*IE (%)*	*CR (mm/y)*	*IE (%)*	*CR (mm/y)*	*IE (%)*
Blank	7.37	-	25.9	-	73.37	-
100	0.90	87.74	5.53	78.63	15.28	84.79
350	-	-	3.80	85.34	-	-
600	1.12	84.79	2.00	92.28	10.25	86.13

Results show that the SB was efficient and significantly reduced the corrosion rate of the alloy. It is clear that the higher the temperature, higher the corrosion rate, either in the presence or absence of the inhibitor. As for the inhibitor concentration, efficiency increases with the SB concentration at 318 and 333 K, but slightly decreases (less than at 3%) at 303 K. Besides, efficiencies are kept above 84% even at 333 K, confirming the protection of the surface by the synthesized compound.

The corrosion rate (CR) is related to the apparent activation energy of the dissolution or carbon steel (E_a) by means of the Arrhenius equation (1):

$$log\ CR = -E_a\,(2.303RT)^{-1} + log\ A \qquad (1)$$

where R is the molar gas constant, T is the absolute temperature and A is a pre-exponential factor. Figure 6 shows the plot results of the logarithm of the corrosion rate (log CR) vs. T^{-1} for carbon steel in 1M HCl in the absence and presence of different concentrations of SB. Straight lines were obtained with a slope of $E_a(2.303R)^{-1}$ from which E_a values were computed. Table III show the values of the activation energies obtained from the plots.

TABLE III. ACTIVATION ENERGIES FOR API P110 CARBON STEEL IN 1M HYDROCLORIC ACID IN THE ABSENCE AND PRESENCE OF SB.

Concentration of SB ($mg \cdot L^{-1}$)	E_a ($kJ\ mol^{-1}$)	R^2
Blank	64.51	0.9994
100	79.38	0.9822
600	65.12	0.9061

The regression coefficients shown in Table III are all above 0.90, suggesting that corrosion of carbon steel can be explained with high certainty using the kinetic model. Higher values of E_a are observed in the presence of the inhibitor in both concentrations, indicating physical adsorption mechanism. Usually, lower E_a values in the inhibiting system than the non-inhibiting indicates chemical adsorption mechanisms, while higher values of E_a in relation to the non-inhibited system indicate physical adsorption mechanism [10]. However, a significant higher value of E_a is noticed for the 100 ppm concentration comparing to the 600 ppm E_a result, which may be associated with greater physical adsorption of molecules to the metallic surface when increasing inhibitor concentration.

Fig. 6. Plots for log(CR) vs. (1/T) for API P110 in 1M HCl in the absence and presence of the SB in two concentrations.

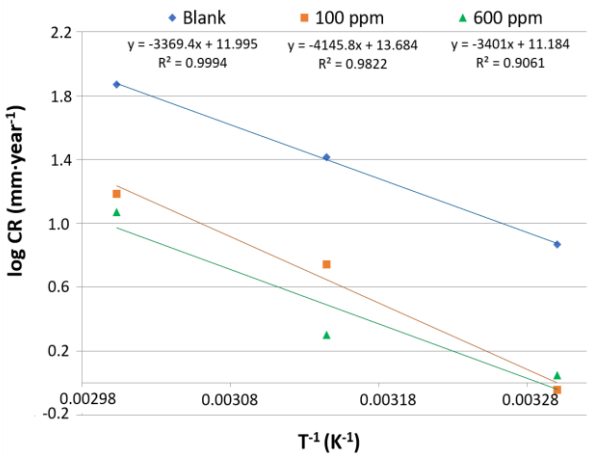

The adsorption of inhibitors can occur through electrostatic interactions between charged species of the inhibitor and the metallic surface (physisorption) or by the chemical interaction between the functional groups of the inhibitor and the metallic orbitals (chemisorption). In order to predict the adsorption mechanism, the fraction of the coated surface (θ) was evaluated in adsorption isotherm models [11]. The models tested were Langmuir, Temkin and El-Awady isotherms, based on the gravimetric data of Table II. The Langmuir isotherm model is expressed by (2) [12],

$$C \cdot \theta^{-1} = K_{ads}^{-1} + C \quad (2)$$

where K_{ads} is the adsorption equilibrium constant and C is the inhibitor concentration. The Langmuir isotherm model best represented the results, with a R^2 value of 0.9952. This informs that the adsorption is characterized by a monolayer coverage of the metal surface. Higher values of K_{ads} indicate better inhibition efficiency and better interaction between species and the metallic surface. However, lower values of K_{ads} indicate that the interactions are weak, and consequently, the adsorbed species can be easily removed by solvent molecules. The value of K_{ads} obtained from the Langmuir isoterm at 318 K was 30.27 $g^{-1}L$. As for the Gibbs free energy change of adsorption, ΔG_{ads}, a value of –19.635 $kJmol^{-1}$ was obtained. The negative value of ΔG_{ads} indicated spontaneous adsorption of the corrosion inhibitor on the carbon steel surface and a strong interaction between the inhibitor molecules and the surface of the steel. Usually, values of ΔG_{ads} around −20 $kJmol^{-1}$ are consistent with physical adsorption, while values around −40 $kJmol^{-1}$ or lower are associated with chemical adsorption, where sharing or transfer of electrons from the organic molecule and the metal atoms of the steel occur [13]. So, the ΔG_{ads} value obtained showed that adsorption of the inhibitor was spontaneous and characterized by physisorption. The Activation Energy values, Ea, obtained from the Arrhenius equation corroborates the physical-type adsorption.

D. Confocal laser scanning microscopy (CLSM)

Confocal laser scanning microscopy was performed in API P110 coupons tested for corrosion in 1M HCl for 24 hours at 318 K in the absence and presence of 600 ppm inhibitor in order to analyze the surface topography and verify any existence of local corrosion. Figure 7 shows the surface microscopy of the blank sample (without inhibitor). Figure 7 (A) shows the 3D surface morphology profile, 7(B) shows the surface topography map and 7(C) shows an image of the surface. Figure 8 shows the surface microscopy of a coupon tested with inhibitor. Pits were observed in the coupons tested with inhibitor, with depths that varied from 9.33 µm (shallow pitting) to 38.7 µm. Figure 8 shows the deepest pitting observed, a shallow-elliptical pitting with 38.7 µm depth (highest value). Figure 8(A) shows the 3D surface morphology profile, 8(B) shows the surface topography map and 8(C) shows an image of the surface.

Fig. 7. Confocal Laser Microscopy of the API P 110 coupon after weight loss test without inhibitor (“blank”).

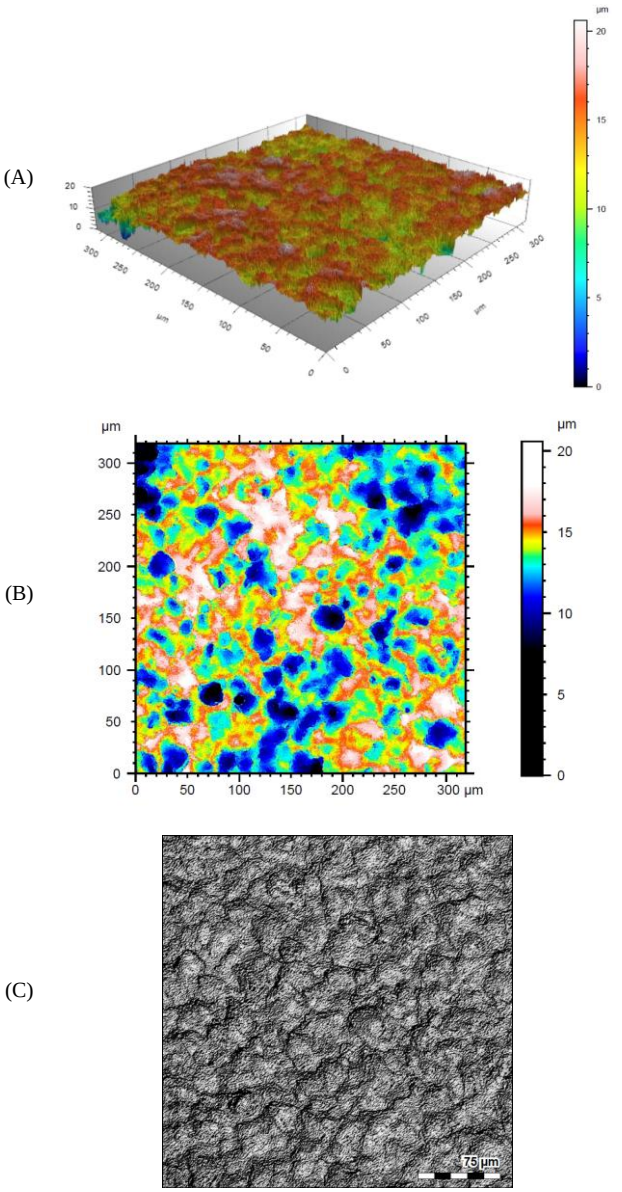

A 38.7 µm depth pitting is considered light to moderate in accordance to ASTM G46 [14]. It is worth mentioning that this work is in development and further improvements in terms of multicomponent formulations will be performed. In this sense, it is expected that the performance of this Schiff base will be improved and localized corrosion reduced in the presence of other compounds in a formulation.

Fig. 8. Confocal Laser Microscopy of the test coupon surface (600 ppm of SB, 318 K).

(A)

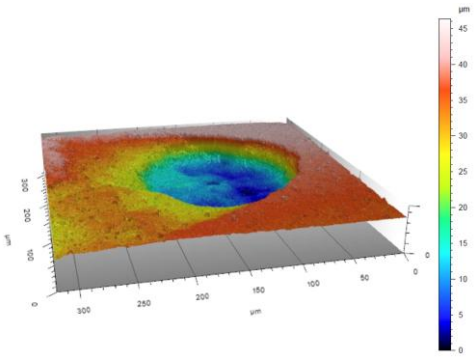

(B)

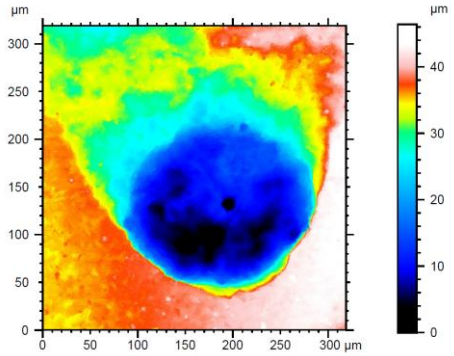

(C)

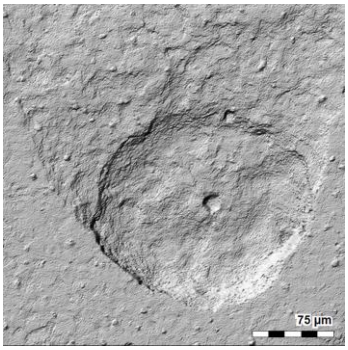

IV. CONCLUSION

The synthesized Schiff base N,N-dimethyl-4-[(phenylimino)methyl]aniline (SB) was prepared by condensation reaction between aniline and 4-(dimethylamino)benzaldehyde. The FTIR spectrum revealed a medium intensity band at 1662 cm^{-1}, referring to the C=N imine bond stretch. The ^{1}H NMR showed a peak for chemical shift of 8.31 ppm that refers to the imine hydrogen, ʃ–N═CH–ʃ. Weight loss results for 24-hour immersions of API P110 test coupons in 1M HCl solutions in the presence and absence of the inhibitor showed that the SB was efficient and significantly reduced the alloy's corrosion rate (CR, mm/y). It was observed that the higher the temperature, higher the corrosion rate, either in the presence or absence of the inhibitor. The best inhibition efficiency obtained from weight loss was 92.28%, achieved by using 600 ppm of SB at 318 K, associated to a CR of 2.00 mm/y. The 2^2 statistical design confirmed that temperature highly influenced the response CR, indicating that concentration of SB is not significant. The Langmuir isotherm model best represented the adsorption results, with a R^2 of 0.9952. So, the adsorption was characterized by a monolayer coverage. The value of K_{ads} obtained was 30.27 $g^{-1}L$ and the Gibbs free energy change of adsorption, ΔG_{ads}, –19.635 $kJmol^{-1}$, which revealed a physical spontaneous mechanism of adsorption. The Activation Energy values, E_a, obtained from the Arrhenius equation corroborates the physical-type adsorption. Confocal laser microscopy showed pits in the coupons tested with inhibitor, with depths related to light/moderate localized corrosion. As this is an ongoing study, further improvements in terms of multicomponent formulations will be performed. So, improvement of the SB performance and reduction of localized corrosion are expected to be achieved.

V. REFERENCES

[1] B. Mokhtar, M. Abdelkader, B. Nora, and N. Mahieddine, "Mild steel corrosion inhibition by Parsley (Petroselium Sativum) extract in acidic media", Egyptian Journal of Petroleum, June 2019, Vol.28(2), 155-159.

[2] H. Ouici, et al., "Adsorption and corrosion inhibition properties of 5-amino 1,3,4-thiadiazole-2-thiol on the mild steel in hydrochloric acid medium: Thermodynamic, surface and electrochemical studies", Journal of Electroanalytical Chemistry, 15 October 2017, Vol.803, pp.125-134.

[3] F. Razieh et al., "Synthesis and potential applications of some thiazoles as corrosion inhibitor of copper in 1 M HCl: Experimental and theoretical studies", Progress in Organic Coatings, July 2019, Vol.132, pp.417-428.

[4] M. M. Solomon, S. A. Umoren, M. A. Quraishi, M. Salman, "Myristic acid based imidazoline derivative as effective corrosion inhibitor for steel in 15% HCl medium", Journal of Colloid And Interface Science, 1 September 2019, Vol.551, pp.47-60.

[5] C. Liang et al., "Synthesis of 2-aminofluorene bis-Schiff base and corrosion inhibition performance for carbon steel in HCl", Journal of Molecular Liquids, 1 March 2019, Vol.277, pp. 330-340.

[6] J. McMurry, "Organic Chemistry", Cengage Learning, 8th Ed., 2012, pp. 973-989.

[7] E. E. Elemike, U. N. Henry, C. O. Damian, E. C. Hosten, "Synthesis, crystal structures, quantum chemical studies and corrosion inhibition potentials of 4-(((4-ethylphenyl)imino)methyl)phenol and (E)-4-((naphthalen-2-ylimino) methyl) phenol Schiff bases", Journal of Molecular Structure, 5 November 2017, Vol.1147, pp. 252-265.

[8] ASTM NACE, American Society for Testing and Materials, ASTMG31-12a, "Standard Guide for Laboratory Immersion Corrosion Testing of Metals", 2012.

[9] D. L. Pavia, G. M. Lampman, G. S. Kriz, J. A. Vyvyan, "Introduction to Spectroscopy", Cengage Learning, 2008.

[10] N. D. Gowraraju, S. Jagadeesan, K. Ayyasamy, L. Olasunkanmi, E. E. Ebenso, C. Subramanian, Journal of Molecular Liquids 232, 2017, 9-19.

[11] E. B. Ituen, A. O. James, O. Akaranta, "Fluvoxamine-based corrosion inhibitors for J55 steel in aggressive oil and gas well treatment fluids", Egyptian Journal of Petroleum 26, 2017, pp. 745-756.

[12] S. P. Cardoso, F. A. Reis, F. C. Massapust, J. F. Costa, L. S. Tebaldi, L. F. L. Araújo, M. V. A. Silva, T. S. Oliveira, J. A. C. P. Gomes, E. Hollauer, Química Nova 28, 2005, 756-760.

[13] A. Y. Musa, A. A. H. Kadhum, A. B. Mohamad, M. S. Takriff, "Molecular dynamics and quantum chemical calculation studies on 4,4-dimethyl-3-thiosemicarbazide as corrosion inhibitor in 2.5 M H2SO4", Mater. Chem. Phys. 2011, 129, 660–665.

[14] ASTM, American Society for Testing and Materials, G46– 94, Standard Guide for Examination and Evaluation of Pitting Corrosion, 2018.